Satellite–Aircraft Handover in Ultra-Dense LEO Satellite Networks

Yilei Wang, *Graduate Student Member, IEEE*, Ting Ma, *Member, IEEE*, Xiaohan Qin, *Student Member, IEEE*, Xin Zhang, *Graduate Student Member, IEEE*, Zitian Zhang, *Member, IEEE*, and Haibo Zhou, *Senior Member, IEEE*

***Abstract*—With the rapid development of low earth-orbit (LEO) satellites, the ultra-dense LEO satellite network (UDLSN) has become a promising solution to provide Internet services for civil aviation due to its wide coverage, exceptional flexibility and high reliability. To guarantee the continuity and high-quality Internet services, satellite-aircraft handover is inevitable because of the high mobility of aircraft and satellites. However, the stringent passenger communication requirements and the considerable increase in the scale of candidate satellites pose huge challenges in satellite-aircraft handover in UDLSNs. In this paper, we investigate multiple civil aircraft handover issue including satellite handover, subchannel allocation, and power selection in the UDLSN and consider different levels of usersâ rate satisfaction, power overhead, and handover overhead as handover criteria for performance measure. The optimization problem is formulated to maximize the handover satisfaction of all civil aircraft. Particularly, the formulated handover problem is represented as a local cooperation game, where each aircraft determines the handover action and the power level by cooperating with other interference aircraft. We prove that the proposed game has at least one Nash Equilibrium (NE) solution in which no aircraft changes its handover strategy. The NE solution in the proposed game is further proven to locally or globally maximize the optimization objective and we then design the parallel handover strategy update (PHSU) algorithm to find the NE solution. Simulation results based on trajectories of real civil aircraft demonstrate that, the designed algorithm is robust, can effectively meet diverse user requirements, and reduce both handover frequency and delays.**

***Index Terms*—Ultra-dense LEO satellite network, civil aviation, satellite handover, power selection, local cooperation game.**

I. Introduction

According to the data released by the International Civil Aviation Organization (ICAO), global air passenger traffic in 2022 increased by 68.5% compared to the previous year [1]. Meanwhile, the communication needs of onboard passengers are becoming increasingly diverse with a growing expectation to experience the same level of Internet connectivity in the air as they do with terrestrial networks. Therefore, the popularization of in-flight Internet service is the future development trend of civil aviation [2], [3]. According to the Union of Concerned Scientists (UCS) satellite database updated on May 1, 2022, the current number of satellites in orbit around the world reached 5,465. Low earth-orbit (LEO) space has become the focus of global space development, ultra-dense low-orbit constellation batch deployment into the peak [4]. A representative case is SpaceX's Starlink program [5], which schedules to deploy a global coverage, high capacity, and low latency space-based global communication system to provide high-speed broadband access services for the world. Thus, ultra-dense LEO satellite networks (UDLSNs) have great potential for providing in-flight Internet services with the future development of the airborne Internet [6], [7]. However, considering the natural mobility of the satellites and aircraft, the satellite-aircraft link handover occurs constantly to ensure the continuity of communication [8], [9]. In addition, the expansion of the LEO satellite constellation scale leads to an increase in the number of the aircraft's candidate satellites. Therefore, a reasonable handover strategy needs to be designed to reduce handover frequency, guarantee the passenger communication demand, and avoid link interruption as well as network congestion [10].

Numerous studies have explored the handover issue in satellite networks. Xu et al. in [11] proposed a quality of service (QoS)-driven intelligent handover mechanism based on the selection of access satellites by predicting service times and communication subchannel resources. Xue et al. in [12] designed a secure authentication protocol and an efficient handover mechanism. It can efficiently reduce the handover delay. To reduce the handover frequency, Kibinda et al. in [13] proposed a handover scheme based on user-centralized collaborative transmission, which captures the irregularities of the cooperative configuration and thus reduces the handover cost. However, the complexity of the handover algorithms is dramatically increasing with the expansion of satellite scale, which is extremely demanding for satellite configuration and adversely affects the handover timeliness [14]. The rapid increase in the number of satellites also leads to an increase in the number of potential overhead satellites for users. Therefore, the execution of handover operations to

Received 20 March 2024; revised 15 July 2024 and 13 September 2024; accepted 15 October 2024. Date of publication 11 November 2024; date of current version 5 March 2025. This work was supported in part by the National Key R&D Program of China under Grant 2020YFB1806104 and the Natural Science Fund for Distinguished Young Scholars of Jiangsu Province under Grant BK20220067. The review of this article was coordinated by Dr. Lin X. Cai. *(Corresponding author: Haibo Zhou.)*

Yilei Wang, Xiaohan Qin, Xin Zhang, and Haibo Zhou are with the School of Electronic Science and Engineering, Nanjing University, Nanjing 210023, China (e-mail: yileiwang@smail.nju.edu.cn; dz20230023@smail.nju.edu.cn; zanxin@smail.nju.edu.cn; haibozhou@nju.edu.cn).

Ting Ma is with the School of Electronic and Optical Engineering, Nanjing University of Science and Technology, Nanjing 210094, China (e-mail: tingma@njust.edu.cn).

Zitian Zhang is with the School of Information and Electronic Engineering, Zhejiang Gongshang University, Hangzhou 310018, China (e-mail: zitian.zhang@mail.zjgsu.edu.cn).

Digital Object Identifier 10.1109/TVT.2024.3495658

ensure users' QoS requirements is also a crucial consideration. Furthermore, most of the preceding studies concentrate on the individual user handover topic, while in practical applications, handover requests are usually initiated by a substantial number of users simultaneously, so it is crucial to examine the multi-user handover issue from a practical perspective. In addition, the interference effects between users have a detrimental impact on passengers' quality of service which requires to be evaluated to ensure the link quality. Moreover, the majority of the existing handover strategies rely on ephemeris data, which lacks robustness and anti-destruction. When there is an unexpected situation such as a satellite malfunction, the accuracy of the handover decision cannot be guaranteed. Based on the above, effective aircraft-satellite link handover decisions in UDLSNs to meet the QoS requirements of multi-aircraft are crucial though difficult [15].

In this paper, inspired by [14], we implement a hierarchical management architecture in UDLSN to cope with surge in network nodes and rapid changes in network topology and guarantee timely network information interaction. Considering civil passengers' service requirements, the difficulty of deploying hardware for airborne communications and the limited satellite resources, civil aviation needs to make a trade-off between economy and the QoS provided to air passengers. Based on the above difficulties, we model the multiple civil aviation aircraft handover, subchannel allocation and power selection problem in UDLSN considering the communication requirements of civil aircraft at various levels. To guarantee the timeliness and effectiveness of the handover implementation, we model the proposed problem as a local cooperative game. We then propose the parallel handover strategy update (PHSU) algorithm to find the Nash equilibrium (NE) solution of the proposed game, which achieves an efficient and reliable handover strategy for civil aviation.

The main contributions are summarised as follows:

- We formulate the downlink handover problem of satellite handover, subchannel allocation, and power selection for multiple civil aircraft in UDLSN. From the perspective of passenger experience and economic benefits, we divide the aircraft into different service levels. Based on this, we construct the handover satisfaction function that consists of three handover criteria (i.e., rate satisfaction, power overhead, and handover overhead) for each aircraft. To satisfy various QoS requirements of aircraft after handover, we define the network utility as the aggregate of all aircraft's handover satisfaction functions. Our goal is to seek a multi-aircraft handover strategy to maximize the network utility.
- We represent the aircraft handover issue as a local cooperative game where aircraft with interference collaborate with each other for handover execution and power selection. We prove the existence of the Nash equilibrium solution for this game which maximizes the network utility locally or globally.
- We design the PHSU algorithm to obtain the NE solution by periodically collecting the interaction information, and each aircraft decides the handover and power allocation policy independently. Meanwhile, we design the handover execution signaling flow to reduce the handover delay. Simulation results verify the PHSU algorithm can meet aircraft's diverse communication requirements, effectively improve the received rate of aircraft and reduce the power overhead. In addition, considering real civil aviation flight trajectory scenarios, the PHSU algorithm illustrates robustness in different scenario configurations.

The subsequent sections of this paper are organized as: Section II describes the related work, Section III presents the scenario depiction, and the problem formulation. Section IV outlines the game analysis, while Section V describes the proposed algorithm. Section VI presents the analytical results. Section VII provides a summary of our work.

II. Related Works

With the flourishing of civil aviation, the demand for in-flight Internet is also increasing, and numerous researchers have studied civil aviation communications in recent years. Wang et al. reveal through comparative simulations in [16] that the time-sensitive resource management performance adopting the dual-link mode in an aviation scenario is only a little superior to that of the single-link mode, but requires more resources and is more sophisticated. Therefore, it is reasonable and meaningful to use single link mode. A channel model was designed for air-space communication using the terahertz band and was evaluated under different conditions in [17]. The results showed that using this model link melting can reach 50-150 Gbps, enabling all passengers on board to have a terrestrial cellular network-like experience during the whole flight. Ultra-dense constellations have become the future trend of satellite networks. Di et al. proposed a hybrid network architecture that combines terrestrial networks and ultra-dense LEO satellites constellations, enabling more efficient data offloading than non-integrated networks [18]. Ma et al. in [14] proposed a multi-layer management architecture for UDLSN with integrated medium-earth-orbit (MEO), LEO, and satellite earth stations, introducing global controllers and local controllers to achieve lightweight management. With the above management architecture, mobility management can be effectively implemented. Based on the above, civil aviation can introduce UDLSN to ensure seamless coverage and guarantee reliable Internet service. Therefore, influenced by [14], we adopt UDLSN as the civil aviation access Internet with a single connection mode and design a combined global and local controller network management architecture to cope with the natural heterogeneity and high dynamics of UDLSN.

Information interaction between aircraft will require higher communication rates, resulting in higher handover frequency. This will increase the network burden and degrade the user experience, which is more evident in UDSLN. Zhou et al. implemented a user-handover operation based on the matching algorithm and modified the particle swarm optimization algorithm to improve the link rate [8]. Jiang et al. proposed a multi-user scheduling algorithm under UDLSN based on the Practical Iterative Subgradient Algorithm, which accelerates the convergence speed and reduces the handover frequency. Existing

handover algorithms designed for terrestrial networks may not be able to handle the dynamic nature of LEO satellite networks. The large scale of satellites creates challenges in managing handovers efficiently and avoiding excessive signaling overhead. What's more, handover algorithms need to consider interference management strategies to ensure seamless handover without degradation in signal quality. All of the above-mentioned points are urgent issues that need to be addressed.

The handover metrics are crucial to the civil passengers' subsequent communication experience and network performance. Currently, many handover algorithms consider handover metrics such as received signal strength (RSS), distance, etc. As the most classic handover metric, RSS is used in [19], [20], [21]. There are also many studies (e.g., [13], [22], [23]) on designing handover algorithms for satellite networks based on link distance. Some other studies collaboratively consider multiple handover metrics to design the handover algorithm. Jia et al. in their paper [20] design a satellite-ground multi-indicators handover method that jointly considers the attributes of link quality, mobility, and throughout, which effectively reduces the number of handovers and improves the network utilization. Qi et al. propose a handover method including track prediction in [21], which considers dwelling time and link quality, available bandwidth, and handover frequency as handover indicators that effectively reduce the number of handovers. However, RSS does not accurately represent the link quality because of the long satellite link distance and large path loss. The distance indicator is very dependent on ephemeris data, and if the satellite is out of order, the relevant information is not available. Therefore, it is critical to choose the appropriate handover indicator in the satellite network to ensure the user service experience and the regular operation of the network.

The implementation of ultra-dense constellations is followed by an upward trend of the network scale's complexity, so it is necessary to carefully select a suitable handover method to cope with the variability and complexity of the network and to ensure the timely and effective execution of the handover. In [24], Zhao et al. suggest a storage strategy, which maps satellite networks to virtual space using digital twins (DTs). To reduce the handover frequency, a satellite-oriented storage handover strategy is presented, which takes into account the access time and satellite capacity. Li et al. analyzed the multilayer satellite network employing the Markov chain in [25] and proposed an improved Markov approximation for the multi- radio access technology selection algorithm, and the results proved that the proposed method can reduce the handover processing time. Gao et al. proposed a game-based handover method in the literature [26]. It outperforms existing solutions in several QoS metrics and effectively solves the data transmission issue when the handover in high-mobility vehicle networks takes place.

Although several handover algorithms have been considered for satellite networks, few studies have been applied to ultra-dense constellation scenarios, and with the expansion of the network scale, the co-channel interference problem will become more sophisticated, which seriously affects the user's communication experience [22]. Therefore, how to consider the handover factors to overcome the complexity and structural variability of the nodes, as well as design a reasonable handover method to guarantee the increasingly demanding communication needs of the users are urgent issues to be addressed [27]. The large scale of UDLSN requires high timeliness of handover algorithms, potential games can handle uncertainty and changes in the environment as they focus on local interactions rather than relying on a global view. This robustness makes them suitable for dynamic and evolving systems. Each player in the cooperative game gains a little more than when it does not cooperate, which facilitates the choice of multi-user handover strategy with interference. Based on the above discussion, we adopt a game approach to design the handover algorithm so as to reduce the complexity of the algorithm and ensure the handover timeliness. Realistically, receive power level can also affect passenger handover performance [28], but is rarely discussed. In addition, the allocation of subchannels and power selection under the influence of link interference can couple to affect the user's communication experience. In the civil aviation scenario, civil aviation companies need to consider economic overheads such as power while providing communication services to passengers. Thus for a better handover strategy and economic factors, we jointly consider link handover, subchannel allocation, and power selection and couple them to enhance the various QoS requirements of aircraft and ensure efficient and robust handover execution in UDLSN. This integrated approach ensures economic efficiency, effective interference management, QoS differentiation, and practical applicability, making it an effective option for addressing the unique challenges of civil aviation handover scenarios.

III. System Model

A. Network Model

As shown in Fig. 1, we demonstrate a classical application scenario of ultra-dense LEO satellite constellations, i.e., an airborne network for civil aviation services. It consists of LEO satellites and user terminals, i.e., civil aircraft. During the mission, the aircraft is equipped with satellite communication equipment that enables a direct connection and visual range communication with LEO satellites. Due to the high-speed movement of the satellite, the connection between the aircraft and the satellite is continuously varying, i.e., handover occurs. To meet the high-capacity communication needs of the passengers on board as much as possible, aircraft need to continuously perform appropriate handover actions to ensure the QoS required by the passengers on board.

We consider the satellite-to-aircraft downlink communication process, which can be extended to uplink scenarios as well. In UDLSN, all LEO satellites share the entire spectrum B pre-divided by the system and the entire spectrum is uniformly divided into K subchannels, each subchannel has the same bandwidth $W = B/K$ [29]. Inspired by work [14], the civil aviation network based on ultra-dense LEO satellites considered in this paper adopts a hierarchical control mechanism, where each MEO satellite acts as the first-level manager of the LEO satellites in its coverage area with maintaining the information table of the LEO satellite constellation and observing the status of the LEO satellites. The LEO satellites in the coverage area

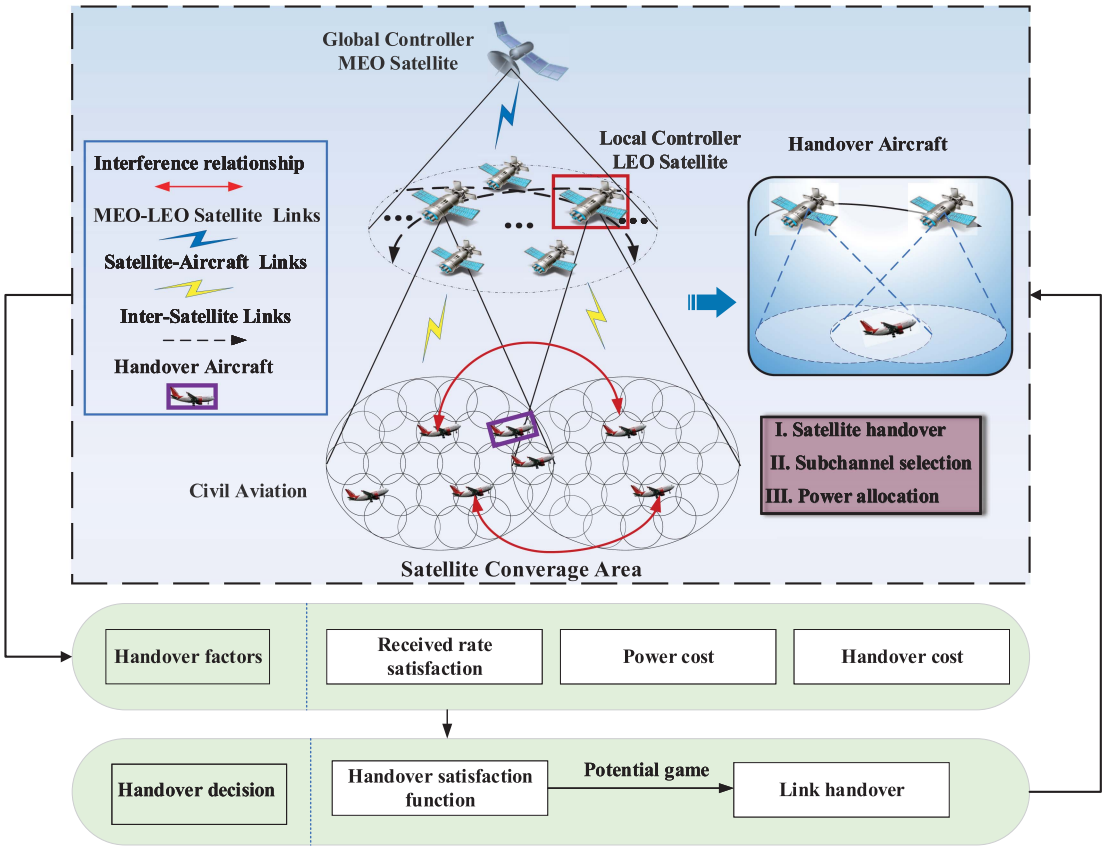

Fig. 1. Hierarchical control of civil aviation Internet handover scenario.

of each MEO satellite are divided into different groups. One LEO satellite in each group is selected as the local controller to manage the flow table of LEO satellites in the same group and is responsible for the content distribution. In the UDLSN, different LEO satellite groups interact with each other via the local LEO satellite controller, and only the local LEO satellite controller can communicate with MEO satellites. Work [14] - [15] and [18] have verified that this two-tier management architecture is effective in reducing the load on the MEO satellites, thus realizing the lightweight management in the UDLSN.

We consider an airspace $\mathcal{R}$ within a period of time $\mathcal{T}$, where $\mathcal{T} = \{1, 2, \ldots, T\}$ and the time interval between adjacent time slots is τ. The set of LEO satellites, aircraft, and subchannels in the system are represented as $\mathcal{N} = \{1, 2, \ldots, N\}$, $\mathcal{M} = \{1, 2, \ldots, M\}$ and $\mathcal{K} = \{1, 2, \ldots, K\}$ respectively. The selected area $\mathcal{R}$ is covered by a MEO satellite, and all LEO satellites in $\mathcal{R}$ are in the same cluster, where one of the LEO satellites is the local controller. The local controller is responsible for maintaining the information of intra-cluster and inter-cluster.

Due to the deployment of an ultra-dense LEO satellite constellation, there are dozens of LEO satellites over the aircraft at all times, so the aircraft handover selection is different from the traditional single strategy selection and should consider various factors such as user demand and economy. In this paper, we consider the user communication requirements and the economic costs of airlines, and choose three factors, namely received rate satisfaction, power overhead, and handover overhead, as the handover indicators to establish the aircraft handover satisfaction function. The specific metrics model is described in detail below.

1) Received Rate Satisfaction: During a flight, each aircraft needs to maintain access a satellite continuously over an idle subchannel to guarantee the continuity of communication. Let the 0-1 variable $x_{m,n}^{k,t}$ represents whether the aircraft m accesses the satellite n over the subchannel k at the t-th moment, i.e., $x_{m,n}^{k,t} = 1$ when the aircraft m accesses the satellite n over the subchannel k at the t-th moment and otherwise $x_{m,n}^{k,t} = 0$. We define that each aircraft can access only one LEO satellite over an available subchannel, while each LEO satellite can communicate with a maximum of K aircraft, i.e.,

$$\sum_{n=1}^{N}\sum_{k=1}^{K} x_{m,n}^{k,t} \leqslant 1,$$
$$\sum_{m=1}^{M}\sum_{k=1}^{K} x_{m,n}^{k,t} \leqslant K. \tag{1}$$

Thus the signal to interference plus noise ratio (SINR) of the aircraft m is connected to the satellite n over the subchannel k at the t-th moment is

$$\Upsilon_{m,n}^{k,t} = \frac{x_{m,n}^{k,t} p_n^{k,t} \left|h_{m,n}^{k,t}\right|^2 \left(d_{m,n}^{t}\right)^{-\sigma}}{\sum_{n' \in \mathcal{N}, n' \neq n} x_{m,n'}^{k,t} p_{n'}^{k,t} \left|h_{m,n'}^{k,t}\right|^2 \left(d_{m,n'}^{t}\right)^{-\sigma} + N_0}, \tag{2}$$

where $p_n^{k,t}$ and $p_{n'}^{k,t}$ are the transmit power of the subchannel k for aircraft m accessing satellite n and satellite n' at moment t, respectively, $d_{m,n}^t$ and $d_{m,n'}^t$ are the distance from aircraft m to satellite n and n' at moment t, respectively, σ is the path loss exponent, N_o is the additive noise power, $N_o \sim \mathcal{CN}(0,\ \sigma_0^2)$, the satellite-to-aircraft link is modeled as Shadowed-Rician fading channels [18], and $h_{m,n}^{k,t}$ and $h_{m,n'}^{k,t}$ are the subchannel gain from the subchannel k of the satellite n and n' to the aircraft m at the moment t, respectively. According to work [7] and [8], we assume that the downlink channel state is known at the beginning of each time slot t and the channel performs flat in each time slot interval τ.

Thus, at the t time slot, the received rate $R_{m,n}^{k,t}$ of the aircraft m is expressed as

$$R_{m,n}^{k,t} = W \log_2 \left(1 + \Upsilon_{m,n}^{k,t}\right). \tag{3}$$

Considering that aircraft belonging to different airlines provide different levels of service and the importance of passengers in-flight are also different, so the received rate requirements of aircraft are not the same. Due to the variation in service levels provided by aircraft from different airlines and the diverse importance of passengers' in-flight needs, aircraft have varying received rate requirements. Accordingly, this paper categorizes the received rate requirements of aircraft into L levels, which are quantified as $\mathcal{R}_{\mathcal{L}} = \{R_o^1, R_o^2, \ldots, R_o^L\}$, then the aircraft rate requirements within the aircraft set $\mathcal{R}_{\mathcal{L}}^{\mathcal{M}} = \{R_o^m | R_o^m \in \mathcal{R}_{\mathcal{L}}, m \in \mathcal{M}, \}$. Define S-Function to denote the user received rate satisfaction situation. Similarly to the meaning of QoE, when the received rate $R_{m,n}^{k,t}$ is lower than the required rate R_o^m, the rate satisfaction grows fast, while when the received rate $R_{m,n}^{k,t}$ is higher than the required rate R_o^m, the rate satisfaction grows slowly. Refer to work [30], the received rate satisfaction S_m^t of aircraft m at the t-th moment is denoted as

$$S_m^t = \sum_{n=1}^{N} \sum_{k=1}^{K} S_{m,n}^{k,t}, \tag{4}$$

where $S_{m,n}^{k,t}$ denotes the received rate satisfaction obtained by the aircraft m accessing the satellite n over the subchannel k at the moment t, which is expressed as

$$S_{m,n}^{k,t} = 1 - e^{-\alpha \frac{R_{m,n}^{k,t}}{R_o^m}}, \tag{5}$$

where α denotes the factor of satisfaction curve steepness. Fig. 2 depicts the variation of the received rate satisfaction with the received rate based on various rate demands and different satisfaction factors. The satisfaction rate takes values from 0 to 1. Furthermore, the marginal rate of satisfaction enhancement is decreasing, which is under the law of diminishing marginal utility in economics. Similarly to work [30], we set $\alpha = 1$.

2) Power Cost: Because civil aviation needs to consider the company's operational issues, the handover choice of the aircraft also needs to consider economic factors. After the aircraft selects a satellite for a certain idle subchannel access, it also needs to pay for the transmit power provided by the satellite, so the airline needs to make a trade-off between the level of service provided to the customer and its own economic overhead. Considering

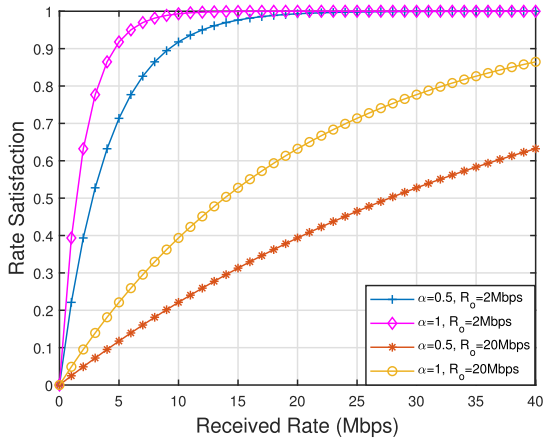

Fig. 2. Received rate satisfaction function for different rate requirements and different satisfaction factors.

the technical cost and resource constraints, only discrete power control is supported for the transmit power in the satellite to aircraft downlink [31]. We define κ_L discrete power choices for the transmit power of each LEO satellite, and the satellite can choose any of the power levels in $\mathcal{P}_{\mathcal{L}} = \{P_L, 2 \cdot P_L, \ldots, \kappa_L \cdot P_L\}$ as the transmit power for a particular subchannel, where P_L is the unit transmit power value. We define the power overhead F-function to denote the power overhead of the aircraft, and at the t-th moment, the power overhead of the aircraft m is denoted as

$$F_m^t = \begin{cases} \pi_2 \left(p_m^t - p_m^{o,t}\right) + \pi_1 p_m^{o,t}, & p_m^t \geqslant p_m^{o,t}; \\ \pi_1 p_m^t, & p_m^t < p_m^{o,t}, \end{cases} \tag{6}$$

where p_m^t is the received power of the aircraft m in the t-th time slot, which is denoted as $p_m^t = \sum_{n=1}^{N} \sum_{k=1}^{K} x_{m,n}^{k,t} p_n^{k,t}$, and $p_{m,n}^{k,t} \in \mathcal{P}_{\mathcal{L}}$. $p_m^{o,t}$ represents the satellite transmit power required when the aircraft m meets the received rate requirement R_o^m in the no-interference state. According to the signal-to-noise ratio (SNR) expression we can obtain that

$$p_m^{o,t} = \frac{\left(2^{\frac{R_o^m}{W}} - 1\right) \cdot N_0}{h_{m,n}^{k,t} \left(d_{m,n}^t\right)^{-\sigma}}, \tag{7}$$

where π_1 and π_2 denote the expenditure coefficients that transform the power overhead into money for the different transmit power cases chosen, respectively. It is clear that $\pi_2 > \pi_1$ and the airline needs to pay a larger economic expenditure for higher power than the threshold value. According to work [32], we set $\pi_1 = 0.01$, $\pi_1 = 0.02$.

3) Handover Cost: Frequent handover between different satellites leads to excessive handover signal overhead, increasing the possibility of network congestion and link interruptions, so the aircraft also needs to consider the handover overhead when carrying out link access. Define the handover overhead of the aircraft m at the t-th moment as C_m^t denoted by

$$C_m^t = \begin{cases} C_o, & x_m^t \neq x_m^{t-1}; \\ 0, & x_m^t = x_m^{t-1}, \end{cases} \tag{8}$$

where $x_m^t \in \mathcal{N}$ denotes the access satellite selection of the aircraft m at the t-th moment and $C_o > 0$ is the fixed handover overhead value. When the satellite accessed by the aircraft at the current moment is different from the satellite accessed at the previous moment, then the handover overhead is generated, otherwise there is no handover overhead.

Considering the economic expenditure as well as user benefits, define the handover satisfaction function of aircraft m at the t-th time slot as

$$\Gamma_m^t = S_m^t - C_m^t - \omega_l \cdot F_m^t, \tag{9}$$

it contains the above three considerations, where ω_l is the weight coefficient of the power cost when the aircraft received rate level is R_o^l and $0 < \omega_l < 1$. ω_l and R_o^l are inversely proportional, i.e., the higher R_o^l, the lower the weighting coefficient ω_l for the power overhead and otherwise the lower R_o^l, the higher ω_l. The adjustment of the weighting coefficients aligns with the principles of market economy, where the aircraft with high service level are willing to pay more to get higher service quality.

B. Problem Formulation

Setting the beginning of each time slot to execute the handover algorithm, thus for the simplicity of expression, we omit the superscript t of $x_{m,n}^{k,t}$, i.e., $x_{m,n}^{k,t} \to x_{m,n}^k$. Define the set of handover actions for the aircraft set $\mathcal{M}$ and the set of power selection actions as $A = \{x_{m,n}^k | m \in \mathcal{M}\}$ and $P = \{p_m | m \in \mathcal{M}\}$, respectively. $x_{m,n}^k, p_m$ are the satellite handover and power selection actions for aircraft m, respectively. The set of action strategy spaces for aircraft m is $\mathcal{A}_m = \{x_{m,n}^k | n \in \mathcal{V}_m, \mathcal{C}_n^k > 0\}$ and $\mathcal{P}_m = \{p_m | m \in \mathcal{M}, p_m \in \mathcal{P}_\mathcal{L}\}$. $\mathcal{V}_m$ is the set of visible satellites of aircraft m, $\mathcal{C}_n^k$ is 0-1 variable, which denotes the state of subchannel k of LEO satellite n and is a criterion for whether aircraft m can access LEO satellite n via subchannel k. $\mathcal{C}_n^k = 0$ means subchannel k of LEO satellite n is occupied and cannot be accessed by other aircraft, and $\mathcal{C}_n^k = 1$ means that the subchannel can be occupied by other aircraft. We characterize the system utility as the satisfaction of the service provided by UDLSN to civil aviation passengers in this airspace, which is expressed as

$$U(A, P) = \sum_{m=1}^{M} \Gamma_m. \tag{10}$$

Our goal is to maximize the satisfaction of service demand received by all aircraft passengers, so we model the optimization problem as

$$(A^*, P^*) = \underset{A \in \mathcal{A}, P \in \mathcal{P}}{arg\ \max}\ U(A, P), \tag{11}$$

where $\mathcal{A}$ and $\mathcal{P}$ are the handover actions for all aircraft and the strategy space for power selection, respectively.

A^* and P^* are the optimal policy solutions of the proposed optimization problem. The strategy space for each aircraft m is $\kappa_L \cdot K \cdot |\mathcal{V}_m|$. The solution set space of the proposed problem is $|\mathcal{V}_1| \cdot |\mathcal{V}_2| \cdots |\mathcal{V}_M| \cdot (\kappa_L K)^M$. Thus, the computational complexity of the optimization goal (11) is $O(N \cdot 2^{|\mathcal{V}_1| \cdot |\mathcal{V}_2| \cdots |\mathcal{V}_M| \cdot (\kappa_L K)^M})$, it is non-polynomial, so the optimization objective belongs to deterministic Polynomial (NP) problem [33]. Thus, it is challenging to find the optimal policy solution by using standard optimization techniques directly. Furthermore, the common optimization methods will lead to exponential growth in time complexity, while the handover problem requires decisions to be made quickly, so we need to design a novel handover algorithm that can handle this high-complexity problem timely and can be applied practically.

IV. Local Cooperation Game for Aircraft Handover

Game theory is a mathematical method for studying phenomena of a struggle or competitive nature. Cooperative games emphasize efficient, fair, and equitable group rationality, where the overall benefit to the cooperative participants will be higher than the sum of the benefits to each participant when operating individually, and each member can gain more than they would have without the cooperation. In this section, we transform the proposed problem (11) into a local cooperative game problem, where each aircraft as a player cooperates with others who have an interference relationship to find the maximum value of the overall benefit, and aircraft who have no interference relationship with each other seek to maximize their handover satisfaction respectively. Then, we prove the proposed game is an exact potential game that has at least one pure strategy NE. The proposed game can reasonably characterize the independent individual properties of strategy interactions and has a strong performance enhancement for hierarchical network architectures.

A. Game Model

We define the players of the local cooperation game as the set of aircraft $\mathcal{M}$. Since there exists interference effects between aircraft, the handover satisfaction of each aircraft will be affected by the handover action of other aircraft. So we present the definition of the potential aircraft interference set $\mathcal{Z}$ to describe the interference relationship between aircraft. The potential aircraft interference set of aircraft m is denoted as

$$\mathcal{Z}_m = \{m' | \exists n \in \mathcal{V}_m, \mathcal{V}_{m'}\}. \tag{12}$$

This suggests that if there exists a LEO satellite n that is both a visible LEO satellite of player m, m', then the two players m, m' have a potential interference relationship, i.e., $m' \in \mathcal{Z}_m$. If player m' is connected to m's visible LEO satellite n' and both players m, m' are connected to the LEO satellite over subchannel k, the downlink from satellite n' to aircraft m' will interfere with aircraft m, so interference relationship is generated between them. According to the definition of $\mathcal{Z}$, if $m' \in \mathcal{Z}_m$, then $m \in \mathcal{Z}_{m'}$. If $m' \notin \mathcal{Z}_m$, there is no interference effect on aircraft m no matter what handover action of aircraft m'. To reasonably characterize the cooperation between the players and allow the cooperation relationship to consolidate and persist, we define that, for each player m, aircraft in the potential aircraft interference set $\mathcal{Z}_m$ are player m's cooperators. Players with potentially interfering relationships can cooperate to minimize the effects of interference between them and thus obtain higher benefits than if they perform the operations individually.

Based on the above cooperative relationships, we define the local cooperative game $\mathcal{G} = \{\mathcal{M}, \{\mathcal{A}_m \otimes \mathcal{P}_m\}_{m \in \mathcal{M}},$

$\{U_m\}_{m\in\mathcal{M}}\}$, where the game players are the aircraft set $\mathcal{M}$, $\mathcal{A}_m \otimes \mathcal{P}_m$ is the handover strategy space of player m, and U_m is the utility function of player m. Considering the resource allocation and benefits assignment among cooperative members, the utility function of player m is defined as

$$U_m\left(a_m, A_{-m}, p_m, P_{-m}\right) = \Gamma_m + \sum_{m'\in\mathcal{Z}_m} \Gamma'_m, \tag{13}$$

where $a_m \in \mathcal{A}_m$ and $p_m \in \mathcal{P}_m$ are the handover decision and power selection action of player m, A_{-m}, P_{-m} denote the handover decisions and power selection actions of players except for participant m, respectively. The utility function of player m contains not only its handover satisfaction but also that of the players within its cooperative set $\mathcal{Z}_m$. This demonstrates that each player needs to consider not only its interests but also the benefits of allied users collaboratively, thus conforming to the actual socioeconomic life system. Then the goal of each player m in the local cooperative game $\mathcal{G}$ to make a strategy choice can be expressed as

$$(\mathcal{G}): \max_{a_m\in\mathcal{A}_m, p_m\in\mathcal{P}_m} U_m\left(a_m, A_{-m}, p_m, P_{-m}\right), \forall m \in \mathcal{M}. \tag{14}$$

Each player chooses a strategy that jointly maximizes its handover satisfaction with the cooperating aircraft, i.e., maximizing the network utility $U(A, P)$, which is equivalent to the optimization problem (11).

B. Game Analysis

NE is a concept of solution in game theory, and this subsection will describe the definition of NE and prove the existence of NE solution for the proposed local cooperative game.

Definition 1 (Nash Equilibrium): A joint profile of handover and power allocation $A^* = (a_m^*, A_{-m}^*, p_m^*, P_{-m}^*)$ is defined as a NE if any one player m chooses a strategy $a_m^* \in \mathcal{A}_m$ that is optimal while all other players A_{-m} stay theirs actions constant, i.e., the following conditions are satisfied

$$\begin{aligned} &U_m\left(a_m^*, A_{-m}^*, p_m^*, P_{-m}^*\right) \geqslant U_m\left(a_m, A_{-m}^*, p_m, P_{-m}^*\right), \\ &\forall m \in \mathcal{M}, \forall a_m \in \mathcal{A}_m \backslash \{a_m^*\}. \end{aligned} \tag{15}$$

This suggests that each player's equilibrium strategy is designed to maximize its utility benefit, while all other players follow such a strategy. In economics, the NE point means that on a certain strategy profile, no player will benefit from changing strategies individually. Therefore, finding the NE point of the proposed game $\mathcal{G}$ means finding the solution to the optimization problem.

Definition 2 (Exact Potential Game): In a game, if there exists a potential function $\Phi \to R$, $\forall m \in \mathcal{M}$, when its strategy $\langle a_m, p_m\rangle \to \langle a'_m, p'_m\rangle$, the actions of other players remain unchanged, the difference of the utility function U_m and the potential function Φ satisfies the following condition,the game is said to be an exact potential game.

$$\begin{aligned} &\Phi\left(a'_m, A_{-m}, p'_m, P_{-m}\right) - \Phi\left(a_m, A_{-m}, p_m, P_{-m}\right) \\ &= U_m\left(a'_m, A_{-m}, p'_m, P_{-m}\right) - U_m\left(a_m, A_{-m}, p_m, P_{-m}\right). \end{aligned} \tag{16}$$

According to the characteristic of an exact potential game, there must be an NE solution for an exact potential game, so we propose Theorem 1 to show that the proposed local cooperative game $\mathcal{G}$ is an exact potential game and design a reasonable potential function Φ to prove Theorem 1.

Theorem 1: The proposed local cooperation game $\mathcal{G}$ is an exact potential game which has at least one pure strategy NE.

Proof: The proof idea is influenced by the paper [30].

First define the potential function Φ of the proposed local cooperation game $\mathcal{G}$ as

$$\Phi(A, P) = \sum_{m=1}^{M} \Gamma_m\left(a_m, A_{-m}, p_m, P_{-m}\right). \tag{17}$$

Based on the definition of the potential interference set $\mathcal{Z}_m$ for aircraft m, we obtain that

$$\Gamma_m\left(a_m, A_{-m}, p_m, P_{-m}\right) = \Gamma_m\left(a_m, A_{\mathcal{Z}_m}, p_m, P_{\mathcal{Z}_m}\right). \tag{18}$$

Propose an information interaction set $\mathcal{D}_m$ definition based on the aircraft m potential interference set $\mathcal{Z}_m$:

$$\mathcal{D}_m = \bigcup_{m'\in\mathcal{Z}_m} \mathcal{Z}_m \cup \mathcal{Z}_{m'}. \tag{19}$$

Player m obtains the value of its utility function U_m by interacting with some players, but not all players and the set of interactions $\mathcal{D}_m$ contains the group of aircraft with whom player m needs to interact. Thus we can simplify the information interaction complexity:

$$U_m\left(a_m, A_{-m}, p_m, P_{-m}\right) = U_m\left(a_m, A_{\mathcal{D}_m}, p_m, P_{\mathcal{D}_m}\right). \tag{20}$$

Based on the above information interaction simplification, we can represent the potential function Φ as

$$\begin{aligned} \Phi(A, P) &= \sum_{m=1}^{M} \Gamma_m\left(a_m, A_{\mathcal{Z}_m}, p_m, P_{\mathcal{Z}_m}\right) \\ &= \Gamma_m\left(a_m, A_{\mathcal{Z}_m}, p_m, P_{\mathcal{Z}_m}\right) + \sum_{i\in\mathcal{Z}_m} \Gamma_i\left(a_i, A_{\mathcal{Z}_i}, p_i, P_{\mathcal{Z}_i}\right) \\ &\quad + \sum_{j\in\mathcal{M}, j\notin\mathcal{Z}_m, j\neq m} \Gamma_j\left(a_j, A_{\mathcal{Z}_j}, p_j, P_{\mathcal{Z}_j}\right). \end{aligned} \tag{21}$$

Denote the potential function Φ as the sum of the utility functions of three types of aircraft including player m, the set of potentially interfering aircraft $\mathcal{Z}_m$ of player m and the remaining aircraft in the user set $\mathcal{M}$.

We can obtain the change in aircraft m's utility function as

$$\begin{aligned} &U_m\left(a'_m, A_{\mathcal{D}_m}, p'_m, P_{\mathcal{D}_m}\right) - U_m\left(a_m, A_{\mathcal{D}_m}, p_m, P_{\mathcal{D}_m}\right) \\ &= \Gamma_m\left(a'_m, A_{\mathcal{Z}_m}, p'_m, P_{\mathcal{Z}_m}\right) + \sum_{i\in\mathcal{Z}_m} \Gamma_i\left(a_i, A'_{\mathcal{Z}_i}, p_i, P'_{\mathcal{Z}_i}\right) \\ &\quad - \Gamma_m\left(a_m, A_{\mathcal{Z}_m}, p_m, P_{\mathcal{Z}_m}\right) - \sum_{i\in\mathcal{Z}_m} \Gamma_i\left(a_i, A_{\mathcal{Z}_i}, p_i, P_{\mathcal{Z}_i}\right). \end{aligned} \tag{22}$$

The potential function changes as

$$\begin{aligned} &\Phi\left(a'_m, A_{-m}, p'_m, P_{-m}\right) - \Phi\left(a_m, A_{-m}, p_m, P_{-m}\right) \\ &= \Gamma_m\left(a'_m, A_{\mathcal{Z}_m}, p'_m, P_{\mathcal{Z}_m}\right) - \Gamma_m\left(a_m, A_{\mathcal{Z}_m}, p_m, P_{\mathcal{Z}_m}\right) \end{aligned}$$

$$+\sum_{i\in\mathcal{Z}_m}\left(\Gamma_i\left(a_i,A'_{\mathcal{Z}_i},p_i,P'_{\mathcal{Z}_i}\right)-\Gamma_i\left(a_i,A_{\mathcal{Z}_i},p_i,P_{\mathcal{Z}_i}\right)\right)$$
$$+\sum_{j\in\mathcal{M},j\notin\mathcal{Z}_m,j\neq m}\left(\Gamma_j\left(a_j,A'_{\mathcal{Z}_j},p_j,P'_{\mathcal{Z}_j}\right)\right.$$
$$\left.-\Gamma_j\left(a_j,A_{\mathcal{Z}_j},p_j,P_{\mathcal{Z}_j}\right)\right). \quad (23)$$

Since only the aircraft handover satisfaction in the potential interference set $\mathcal{Z}_m$ of aircraft m changes regardless of the player m's policy, while other aircraft are unaffected, thus

$$\Gamma_j\left(a_j,A'_{\mathcal{Z}_j},p_j,P'_{\mathcal{Z}_j}\right)=\Gamma_j\left(a_j,A_{\mathcal{Z}_j},p_j,P_{\mathcal{Z}_j}\right),$$
$$\forall j\in\mathcal{M},j\notin\mathcal{Z}_m,j\neq m. \quad (24)$$

Then the change in the potential function can be expressed as

$$\Phi\left(a'_m,A_{-m},p'_m,P_{-m}\right)-\Phi\left(a_m,A_{-m},p_m,P_{-m}\right)$$
$$=\Gamma_m\left(a'_m,A_{\mathcal{Z}_m},p'_m,P_{\mathcal{Z}_m}\right)+\sum_{i\in\mathcal{Z}_m}\Gamma_i\left(a_i,A'_{\mathcal{Z}_i},p_i,P'_{\mathcal{Z}_i}\right)$$
$$-\Gamma_m\left(a_m,A_{\mathcal{Z}_m},p_m,P_{\mathcal{Z}_m}\right)-\sum_{i\in\mathcal{Z}_m}\Gamma_i\left(a_i,A_{\mathcal{Z}_i},p_i,P_{\mathcal{Z}_i}\right). \quad (25)$$

Based on the above analysis we conclude that when any player m changes its strategy arbitrarily, we can obtain that

$$U_m\left(a'_m,A_{\mathcal{D}_m},p'_m,P_{\mathcal{D}_m}\right)-U_m\left(a_m,A_{\mathcal{D}_m},p_m,P_{\mathcal{D}_m}\right)$$
$$=\Phi\left(a'_m,A_{-m},p'_m,P_{-m}\right)-\Phi\left(a_m,A_{-m},p_m,P_{-m}\right). \quad (26)$$

Thus Theorem 1 is proved.

Theorem 2: The NE of the proposed game $\mathcal{G}$ can maximize the network utility locally or globally.

Proof: All NEs are either the local or global maximizing individuals of the potential function Φ, according to D. Monderer and L. S. Shapley [34]. As stated in the definition of network utility, it is known that the network utility is the sum of handover satisfaction of overall aircraft, which is the same as the description of the proposed game's potential function, thus the NE of the proposed game $\mathcal{G}$ can maximize the network utility locally or globally. Hence Theorem 2 is proved and it is worth noting that the best NE solution is the optimal solution that maximizes the network utility value.

V. Algorithm Design for Finding NEs

In this section, we propose parallel handover strategy update algorithm to obtain NE solutions. Under the hierarchical control mechanism, civil aircraft can make the handover decision autonomously based on the satellite-related information, and its convergence is faster and less complex, which is suitable for scenarios with high requirements on time efficiency.

A. Parallel Handover Strategy Update (PHSU) Algorithm

Several approaches to find NEs for potential games have been proposed, such as best response dynamic [35], fictitious play [36], and no-regret learning [37]. However, they all aim to achieve equilibrium solutions and are prone to fall into undesired equilibria. In recent years, γ-logit methods [38] have attracted a lot of attention in potential game theory due to their good equilibrium selection and the nature of exploring the global optimum. Therefore influenced by the γ-logit method we propose the PHSU algorithm to find the NE solution.

Algorithm 1: Parallel Handover Strategy Update Algorithm.

Input: Initial the iteration $e=0$ and $\forall m\in\mathcal{M}$ randomly selects a visible satellite and a idle subchannel a_m to handover and also chooses a random transmit power level p_m.

Output: Uplink handover selection and power allocation policy (A^*,P^*).

1: **for** Loop $e=1,\ldots,L_e$ **do**
2: A group of non-interfering players $m_1,m_2\in\mathcal{N}_e$ is randomly selected, where $\forall m_1,m_2\in\mathcal{M},m_1\notin\mathcal{D}_{m_2}$;
3: $\forall m\in\mathcal{N}(e)$ calculates its utility function $U_m(e)$ by (13);
4: Each player m randomly selects a handover strategy $\{a_m^f,p_m^f\}$ in $\{\mathcal{A}_m^e,\mathcal{P}_m^e\}$;
5: Through interacting with players in $\mathcal{Z}_m$, each player m calculates the utility function value of exploration $U_m^f(e)$;
6: Each player m calculates the policy update probability $\pi_m(e)$;
7: Each player m updates its action according to the rule $\pi_m(e)$. Meanwhile, other players keep the original method unchanged, i.e., $\{a_{m'}(e),p_{m'}(e)\}=\{a_{m'}(e-1),p_{m'}(e-1)\},\forall m'\in\mathcal{M},m'\notin\mathcal{N}_e$
8: **if** Convergence condition reached **then**
9: break
10: **else**
11: $e=e+1$.
12: **end if**
13: **end for**

In each iterative e, the strategy chosen by player m is defined as $\{a_m(e),p_m(e)\}$. To speed up the computation, a set of players $m_1,m_2\in\mathcal{N}_e$ that do not interfere with each other can be updated iteratively in parallel, i.e., $m_1\notin\mathcal{D}_{m_2}$ and $m_2\notin\mathcal{D}_{m_1}$. During the exploration phase, player m can randomly select a handover strategy $\{a_m^f,p_m^f\}$ from the set of actions $\{\mathcal{A}_m^e,\mathcal{P}_m^e\}$. It only needs to interact with its cooperative aircraft $\mathcal{Z}_m$ to compute the exploration utility function value $U_m^f(e)$ without global message delivery, which greatly reduces the signaling interaction overhead and algorithm complexity. Based on the exploration utility value $U_m^f(e)$ and the utility value $U_m(e)$ obtained by the current iterative e, the following policy update rules are used to perform the policy update.

$$\pi_m(e)=\begin{cases}\frac{e^{\mu U_m^f(e)}}{e^{\mu U_m^f(e)}+e^{\mu U_m(e)}}, & s_m(e)=s_m^f(e);\\ \frac{e^{\mu U_m(e)}}{e^{\mu U_m^f(e)}+e^{\mu U_m(e)}}, & s_m(e)=s_m(e),\end{cases} \quad (27)$$

where $s_m(e)$ denotes $\{a_m(e),p_m(e)\}$, $s_m^f(e)$ denotes $\{a_m^f(e),p_m^f(e)\}$ and μ is the exploration factor. The smaller μ

is, the more the aircraft tends to explore more strategy options. For other players $\forall m' \in \mathcal{M}, m' \notin \mathcal{N}_e$, their strategy remains the same: $\{a_{m'}(e+1), p_{m'}(e+1)\} = \{a_{m'}(e), p_{m'}(e)\}$.

This iterative process is explored cyclically until the convergence condition is reached. Algorithm 1 contains information about the PHSU algorithm in detail.

Theorem 3: If all players use the proposed policy update algorithm, the unique stationary distribution of any handover policy is

$$\pi(A,P) = \frac{e^{\mu\Phi(A,P)}}{\sum_{\{A,P\}\in\{\mathcal{A},\mathcal{P}\}} e^{\mu\Phi(A,P)}}. \tag{28}$$

Proof: We define the system handover policy in the iterative e as $\{A(e), P(e)\}$, and we know that $\{A(e), P(e)\}$ is a discrete Markov process. Therefore, it has a unique stationary distribution. We define any iterative process e in which two systematic random policy transitions select states $S = \{A, P\}, S' = \{A', P'\}$, where $A = \{a_1, a_2, \ldots, a_{|\mathcal{N}_e|}, a_{|\mathcal{N}_e|+1}, \ldots, a_M\}$, $A' = \{a'_1, a'_2, \ldots, a'_{|\mathcal{N}_e|}, a_{|\mathcal{N}_e|+1}, \ldots, a_M\}$, $P = \{p_1, p_2, \ldots, p_{|\mathcal{N}_e|}, p_{|\mathcal{N}_e|+1}, \ldots, p_M\}$, $P' = \{p'_1, p'_2, \ldots, p'_{|\mathcal{N}_e|}, p_{|\mathcal{N}_e|+1}, \ldots, p_M\}$. Assume that the probability of the selected player updating the policy is ϵ, then

$$\pi(S)P(S'|S) = \frac{e^{\mu\Phi(S)}}{\sum_{S\in\mathcal{S}^e} e^{\mu\Phi(S)}} \cdot \frac{\epsilon}{\kappa_L} \cdot \prod_{m\in\mathcal{N}_e} \frac{e^{\mu U_m\left(a'_m, A'_{\mathcal{D}_m}, p'_m, P'_{\mathcal{D}_m}\right)}}{e^{\mu U_m(a_m, A_{\mathcal{D}_m}, p_m, P_{\mathcal{D}_m})} + e^{\mu U_m\left(a'_m, A'_{\mathcal{D}_m}, p'_m, P'_{\mathcal{D}_m}\right)}}. \tag{29}$$

We can rewrite it as

$$\pi(S)P(S'|S) = \frac{\epsilon}{\kappa_L \sum_{S\in\mathcal{S}^e} e^{\mu\Phi(S)}} \cdot \prod_{m\in\mathcal{N}_e} \frac{1}{e^{\mu U_m(a_m, A_{\mathcal{D}_m}, p_m, P_{\mathcal{D}_m})} + e^{\mu U_m\left(a'_m, A'_{\mathcal{D}_m}, p'_m, P'_{\mathcal{D}_m}\right)}} \cdot e^{\mu\Phi(S)+\mu\sum_{m\in\mathcal{N}_e} U_m\left(a'_m, A'_{\mathcal{D}_m}, p'_m, P'_{\mathcal{D}_m}\right)}. \tag{30}$$

For the concise presentation, we define

$$\kappa = \frac{\epsilon}{\kappa_L \sum_{S\in\mathcal{S}^e} e^{\mu\Phi(S)}} \cdot \prod_{m\in\mathcal{N}_e} \frac{1}{e^{\mu U_m(a_m, A_{\mathcal{D}_m}, p_m, P_{\mathcal{D}_m})} + e^{\mu U_m\left(a'_m, A'_{\mathcal{D}_m}, p'_m, P'_{\mathcal{D}_m}\right)}}. \tag{31}$$

Thus we state that

$$\pi(S)P(S'|S) = \kappa \cdot e^{\mu\Phi(S)+\mu\sum_{m\in\mathcal{N}_e} U_m\left(a'_m, A'_{\mathcal{D}_m}, p'_m, P'_{\mathcal{D}_m}\right)}. \tag{32}$$

Analogously, we can see that

$$\pi(S')P(S|S') = \kappa \cdot e^{\mu\Phi(S')+\mu\sum_{m\in\mathcal{N}_e} U_m(a_m, A_{\mathcal{D}_m}, p_m, P_{\mathcal{D}_m})}. \tag{33}$$

We define that

$$1 \le i \le |\mathcal{N}_e|, S_i = \left\{\{a'_1, \ldots, a'_i, a_{i+1}, \ldots, a_M\}, \left\{ p'_1, \ldots, p'_i, p_{i+1}, \ldots, p_M \right\}\right\}.$$

Then $S' = S_{|\mathcal{N}_e|}$, it is seen that

$$\begin{aligned} &\Phi(S') - \Phi(S) \\ &= \Phi\left(S_{|\mathcal{N}_e|}\right) - \Phi(S) \\ &= \sum_{m\in\mathcal{N}_e} \left(\Phi(S_m) - \Phi(S_{m-1})\right) \\ &= \sum_{m\in\mathcal{N}_e} \left(U_m(S_m) - U_m(S_{m-1})\right). \end{aligned} \tag{34}$$

$\forall m \in \mathcal{N}_e$, they are non-interfering aircraft of each other, and the policy results do not affect each other, so

$$\begin{aligned} &\Phi(S') - \Phi(S) \\ &= \sum_{m\in\mathcal{N}_e} \Big(U_m\left(a'_m, A'_{\mathcal{D}_m}, p'_m, P'_{\mathcal{D}_m}\right) \\ &\qquad - U_m(a_m, A_{\mathcal{D}_m}, p_m, P_{\mathcal{D}_m}) \Big). \end{aligned} \tag{35}$$

According to (32) and (33), we can obtain

$$\pi(S)P(S'|S) = \pi(S')P(S|S'). \tag{36}$$

Therefore, we draw the derivation

$$\begin{aligned} &\sum_{S\in\mathcal{S}} \pi(S)P(S'|S) = \sum_{S\in\mathcal{S}} \pi(S')P(S|S') \\ &= \pi(S') \sum_{S\in\mathcal{S}} P(S|S') = \pi(S'), \end{aligned} \tag{37}$$

where $\mathcal{S}$ is handover strategy space for all players.

Since the proposed PHSU algorithm has a unique stationary distribution and the given distribution satisfies its Markov process's equilibrium equation. We can conclude that its stationary distribution must be (28). Thus, Theorem 3 is proved.

Theorem 4: When μ is sufficiently large, the PHSU algorithm achieves the globally optimal solution of maximizing the system utility value issue with arbitrarily high probability.

Proof: We define $\{A^*, P^*\}$ to be the optimal solution of the proposed problem, which is the pure NE solution of the proposed local cooperative game $\mathcal{G}$ according to the proven Theorem 2, so we can obtain

$$(A^*, P^*) = \underset{A\in\mathcal{A}, P\in\mathcal{P}}{arg\,max}\ \Phi(A,P). \tag{38}$$

Thus when $\mu \to \infty$, $e^{\mu\Phi(A^*,P^*)} \gg e^{\mu\Phi(A',P')}$, $\{A', P'\} \in \{\mathcal{A}, \mathcal{P}\} \backslash \{A^*, P^*\}$. So according to the probability distribution of Theorem 3 we know

$$\lim_{\mu\to\infty} \pi(A^*, P^*) = 1. \tag{39}$$

It is shown that the proposed algorithm converges to the global optimum with arbitrarily high probability.

Complexity: In each iteration, the complexity for each aircraft m to compute their handover satisfaction is $\mathcal{O}(|\mathcal{Z}_m|)$, and thus the complexity to obtain the aircraft's utility function is $\mathcal{O}(|\mathcal{Z}_m|^2)$. While the total complexity of the PHSU algorithm is also related to the number of convergences, which is coupled with the algorithm performance, it will be analyzed in the simulation. The PHSU algorithm's complexity is greatly reduced

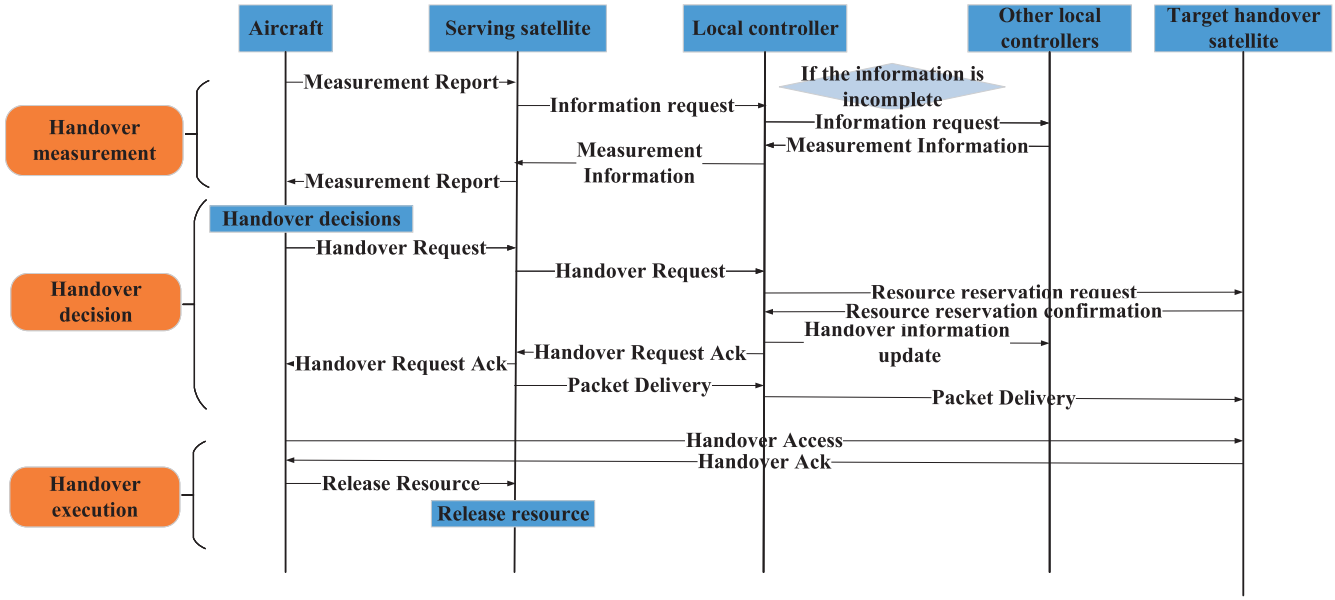

Fig. 3. PHSU algorithm execution signaling process.

compared to the computational complexity of the original problem $\mathcal{O}(N \cdot 2^{|\mathcal{V}_1|\cdot|\mathcal{V}_2|\cdots|\mathcal{V}_M|\cdot(\kappa_L K)^M})$, which alleviates the computational power requirements and improves the time efficiency.

B. PHSU Algorithm Procedure

Fig. 3 illustrates the execution process of the PHSU algorithm, which is mainly divided into three parts: handover measurement, handover decision, and handover execution. First, in the handover measurement phase, the aircraft periodically sends a measurement report to the current access satellite and the measurement report consists the relevant information needed to make the handover decision. If the local controller has incomplete information, it further interacts with other local controllers to obtain all the required measurement information. After receiving the request, the local controller performs resource reservation confirmation to ensure that the aircraft can handover, returns Ack information, and synchronizes the handover information to other local controllers. After the current access satellite receives the Ack information, if there are any uncompleted packets, they are submitted to the target handover LEO satellite through the local controller. Finally, the aircraft executes the handover action, and after the handover is completed, the previous access satellite releases the resources.

It is worth noting that the measurement information required for handover is usually stored in the local controller that manages the current access satellite. When it is necessary to interact with other local controllers for information required for making handover decisions, the interaction delay is also within a few milliseconds, so the signaling interaction delay for obtaining the measurement information is very short and no information delay affects the accuracy of the handover decision.

Therefore, according to the signaling process, the handover delay T_h is defined by

$$T_h = T_s + 2 \times T_{hd} + 2 \times T_{he} + T_p, \tag{40}$$

where T_s is the processing delay for the aircraft to make the handover decision, T_{hd} is the signaling delay required for the aircraft to report the handover request to the local controller during the handover decision phase, T_{he} is the delay for handover to the target satellite during the handover execution phase, and T_p is the packet transmission delay.

VI. Numerical Simulations

In this section, we select the trajectory of the aircraft over the Indian Ocean in the Europe-North America East Coast route for simulation to analyze the performance of the PHSU algorithm [39]. We choose different phases of Starlink constellation configuration as the satellite access network for civil aviation and evaluate the performance obtained by the PHSU algorithm for different cases. To verify the superiority of the PHSU algorithm from multiple perspectives, we compare the PHSU algorithm with two benchmark algorithms commonly used for handover, i.e., maximum rate (MR) algorithm and shortest distance (SD) algorithm. The MR algorithm's rule is accessing the LEO satellite which can provide the maximum received rate for the aircraft and the SD algorithm's rule is selecting the LEO satellite with the shortest distance from the aircraft. Other detailed simulation settings are listed in Table I.

A. Convergence

Considering the limited resources on the satellites, we set Starlink's phase I of 4,408 LEO satellites to provide communications services for civil aviation. The number of aircraft in the simulation is 100 and the number of aircraft with the received rate requirement R_o^1 and R_o^2 is 10 and 90 respectively.

TABLE I
SIMULATION PARAMETERS

Parameter	Value
The additive Gaussian noise variance σ^2	−174 dBm/Hz
The total bandwidth of LEO satellites B	600 MHz
Number of civil aviation aircraft levels L	2
The received rate requirements R_o^1, R_o^2	20 Mbps, 2 Mbps
Number of received power levels κ_L	3
The unit transmit power P_L	100 mW
Handover cost C_o	0.5
Weighting factors ω_1, ω_2	0.2, 0.3
The processing delay T_s	10 ms

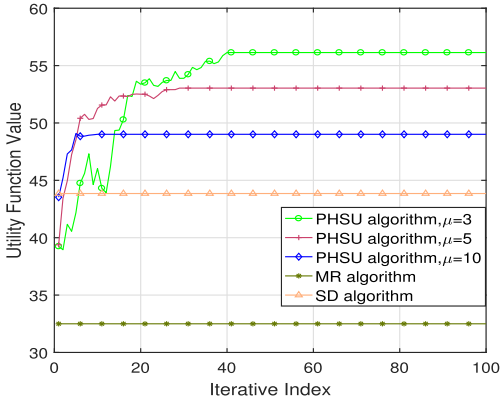

Fig. 4. Convergence performance comparison at different μ cases.

Fig. 4 depicts the convergence tendency of the PHSU algorithm with different updating parameters. It indicates that, when the learning rate is set to a larger value, it can accelerate the convergence process, but the performance of the obtained solution is relatively poor, in contrast to the previous case, with a small learning rate, it converges towards a better solution, but the convergence speed is slow. We can observe that, the convergence rate of $\mu = 5$ is very close to that of $\mu = 10$, while the former obtains better network utility than the latter. In addition, the performance of $\mu = 5$ is close to the performance of $\mu = 3$ which is the optimal in above three cases. Thus, to balance convergence speed and solution quality, we set $\mu = 5$ in follow-up simulations. The network utilities obtained by the two benchmark algorithms are also given in Fig. 4, which are much lower than to that of the PHSU algorithm.

To further explore the robustness of our algorithm, we simulated scenarios where some links suddenly disconnect. As shown in the Fig. 5, the algorithm initially reaches a stable state after 26 iterations. When some links disconnect at the 57th iteration, the algorithm re-iterates and reaches a new Nash equilibrium at the 82-th iteration. Similarly, during the second convergence phase, another link disconnection occurs, and the algorithm again quickly converges after 22 iterations. These results demonstrate that our algorithm can swiftly adapt to topology changes, highlighting its robustness in dynamic environments.

B. Performance Analysis

For more performance analysis, we set the number of available subchannels of each LEO satellite to 15. To prevent network congestion, we set the number of reserved subchannels of each

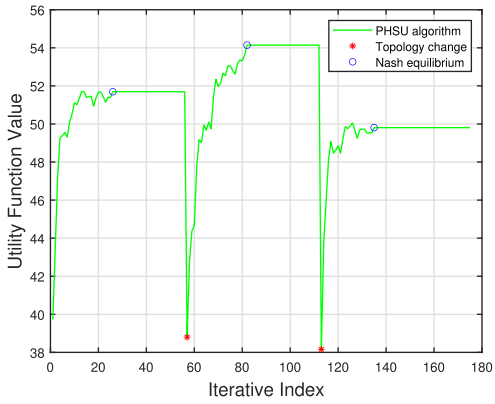

Fig. 5. Convergence performance of the PHSU algorithm under dynamic scenario.

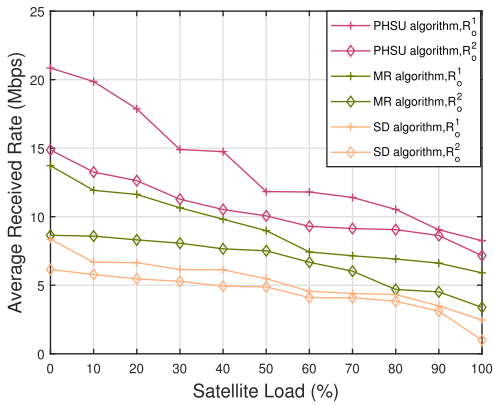

Fig. 6. The average received rate obtained by PHUS, MR, and SD algorithms.

LEO satellite to 5. Define the satellite load as the ratio of the number of occupied subchannels of each LEO satellite to the total number of subchannels except the reserved subchannels. To show the superiority of the PHSU algorithm, we compare it with two benchmark algorithms in terms of the aircraft's received rate and the transmit power for different satellite load cases.

Fig. 6 describes the average received rate with different aircraft's priority levels. Manifestly, the aircraft's received rate decreases overall with the increase of satellite load, because as the satellite resources become congested, the aircraft's options are reduced accordingly. However, high-priority aircraft are more willing to pay more economic overhead to obtain a higher quality of services, so they obtain higher received rates than low-priority aircraft. The PHSU algorithm obtains the best overall rate results, because the PHSU algorithm takes into account the interference among aircraft, and it can cooperate with the handover aircraft to obtain higher received rate satisfactions as much as possible, thus, the received rate of cooperated aircraft can be improved. As a contrast, the MR algorithm does not consider the interference effect, which leads to a low received rate. The SD algorithm only considers the distance factor and does not consider the subchannel quality, so the lowest received rate is obtained.

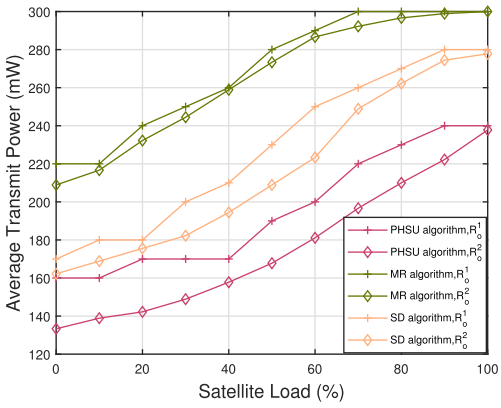

Fig. 7. The average transmit power obtained by PHUS, MR, and SD algorithms.

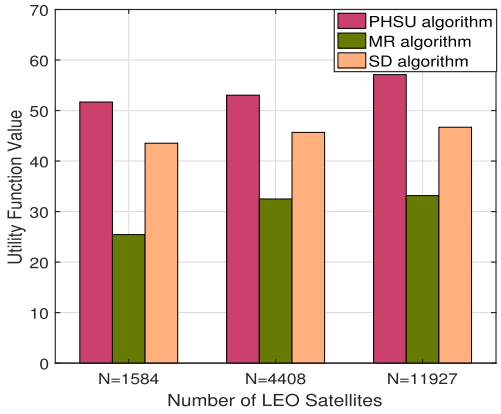

Fig. 8. The network utility value at different satellite network scales.

Fig. 7 displays the average downlink transmit power of different priority aircraft. The more congested the network is, the higher downlink transmit power aircraft need to get better communication quality. Hence, the average transmit power is proportional to the satellite load. High-priority aircraft have higher rate requirements, so they need higher transmit power than low-priority aircraft. We can observe that, the MR algorithm requires the highest transmit power because the MR algorithm aims to obtain the highest SNR value. Therefore, the MR algorithm prefers to choose a high power value, while the SD algorithm does not care about the power overhead and randomly selects the power value. The PHSU algorithm incorporates the power overhead into the optimization index so that the aircraft will choose the low power value as much as possible. As a result, the PHSU algorithm reduces the transmit power value and can obtain the lowest power overhead.

C. Impact of Satellite Scale

With the explosion of LEO satellites, it is essential to investigate the optimal LEO satellite network scale for civil aviation. Thus, we simulate and analyze the service performance in civil aviation at different phases of Starlink's constellation scale.

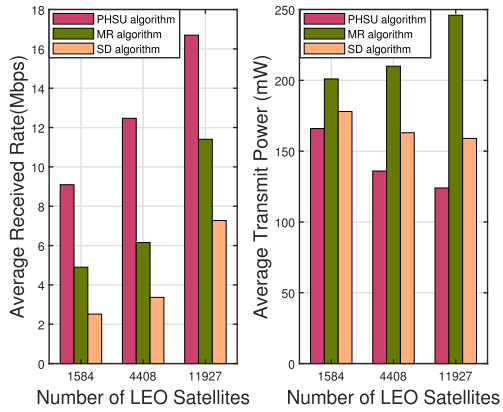

Fig. 9. The average rate and transmit power at different satellite network scales.

Fig. 8 shows the network utilities obtained by PHSU, MR and SD algorithms with different satellite constellation scales. Notably, the network utility value obtained by the PHSU algorithm grows when the LEO satellite constellation scale gets bigger and is always the optimal. While the performances obtained by the MR algorithm and SD algorithm are not proportional to the number of the LEO satellites. This is because when the satellite scale increases, the aircraft's strategy space expands, so worse handover strategies emerge. Both the two benchmark consider only a single indicator, which is easy to fall into the strategy trap and choose a worse handover strategy. Thus, it is clear that the classical single indicator handover algorithm is not well applicable for UDLSN.

Fig. 9 shows the average rates and transmit power values obtained by all the three algorithms. With the satellite scale increasing, the average aircraft received rate obtained by the PHSU algorithm shows an increasing trend and the average transmit power shows a decreasing trend. This shows that providing a larger number of LEO satellites to serve civil aviation could effectively improve the quality of communication for users and reduce power overhead. Moreover, the PHSU algorithm admits the best performance for all constellation sizes, which reflects the adaptability and flexibility of the PHSU algorithm.

D. Impact of Aircraft Number

The number of civil aviation flights can fluctuate up and down due to holidays and other reasons. Therefore, it is desirable to discuss the effect of aircraft density on performance in airspace. Fig. 10 depicts the impact of the number of aircraft on the three algorithms.

From Fig. 10, the PHSU algorithm can always obtain the best utility function value and admits an increasing trend with the increase of aircraft number. When the amount of aircraft is small, the network utilities derived by the MR algorithm and SD algorithm are both inversely correlated with the number of aircraft. But when the number of aircraft is larger, the MR algorithm as well as the SD algorithm shows unsuitability, and the utility function value appears a decreasing trend successively. This is because the co-channel interference becomes more serious with

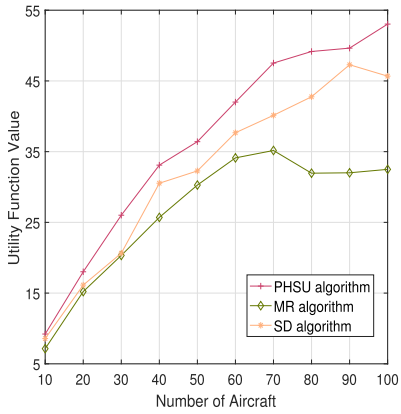

Fig. 10. The network utility value at different civil aircraft numbers.

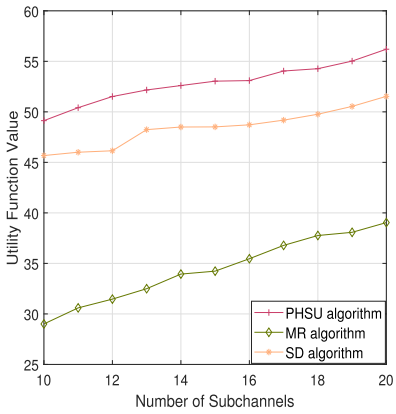

Fig. 11. The network utility value at different subchannel numbers.

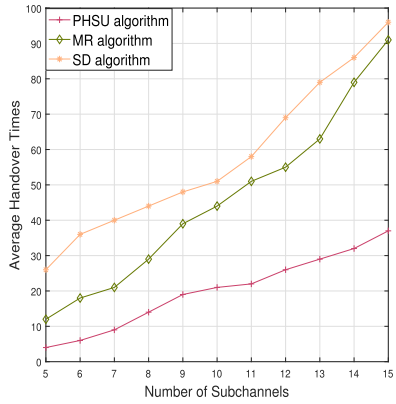

Fig. 12. The handover frequency at different subchannel numbers.

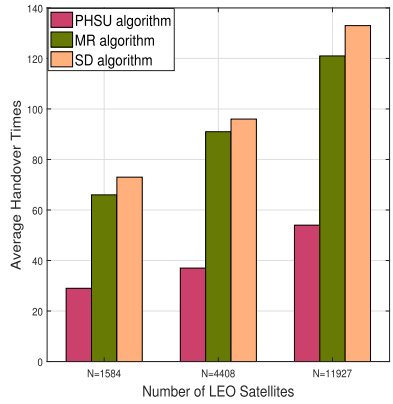

Fig. 13. The handover frequency at different satellite network scales.

the number of aircraft increasing. The interference between aircraft becomes severe with the number of aircraft increasing. The performance obtained by the MR algorithm starts to fluctuate first because the MR algorithm only considers SNR, so it is severely affected. Since the SD algorithm prefers to select the nearest satellite within a short period and generally maintains the current strategy as much as possible, so the performance drops slightly later than the performance of the MR algorithm, i.e., the network utility obtained by the SD algorithm starts to fall when the number of aircraft is 90, while the network utility obtained by the MR algorithm starts to fall when the number of aircraft is 70. It can be seen that the PHSU algorithm can make the multi-aircraft handover decision considering the influence of interference. On the contrary, the performance of the PHSU algorithm keep increasing when the aircraft number gets larger, which reflects the robustness of the PHSU algorithm.

E. Impact of Subchannel Number

The number of subchannels is closely related to the interference among aircraft. Fig. 11 shows the utility function values obtained by the three algorithms with different numbers of subchannels. Manifestly, the utility function values obtained by the PHSU algorithm grow with the increasing number of subchannels and always outperform the two benchmark algorithms. The network utility values obtained by the MR algorithm and SD algorithm show larger fluctuations than the PHSU algorithm with the increase of subchannel numbers. It indicates that the two algorithms do not consider the influence of interference and are highly influenced by environmental factors. Thus, they are not robust and cannot adapt to the dynamic changes of aircraft and the UDLSN. It further demonstrates that the PHSU algorithms can adapt to the complex policy space and make optimal handover decisions.

F. Handover Frequency

The handover frequency is an important indicator to judge a handover strategy. If handover occurs frequently, the interruption probability will greatly increase, which affects the user's service experience. We simulate the aircraft's average handover times of the three algorithms for 30 minutes. Figs. 12 and 13 analyze the effect of different available subchannel numbers and different satellite network scales on the handover times, respectively. It can be seen that, as the number of available subchannels or satellites increases, the choice of handover strategies increases, and therefore the handover times increase. The PHSU algorithm obtains the smallest handover times, which is much lower than the other two benchmark algorithms. This is because the PHSU algorithm takes into account the handover overhead and can minimize unnecessary handover. The MR algorithm requires the aircraft to always choose the satellite with the largest SNR to handover, and the SD algorithm needs to constantly

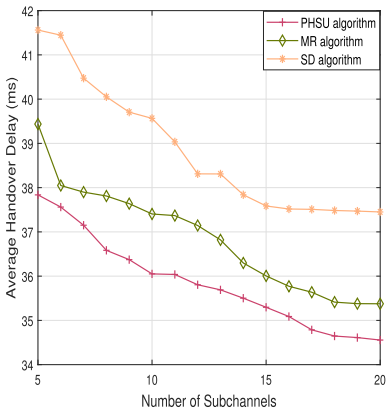

Fig. 14. The handover delay at different subchannel sizes.

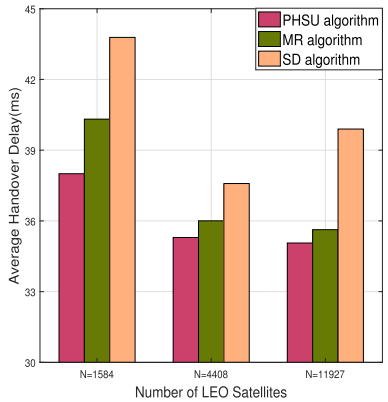

Fig. 15. The handover delay at different satellite sizes.

change the access satellite to the closest satellite. The MR and SD algorithms do not consider the handover cost, so the handover times are much higher than the PHSU algorithm. Additionally, the handover frequency fluctuates more slowly with the change in the number of subchannels and LEO satellites compared with the two benchmark algorithms, which reflects the robustness of the PHSU algorithm.

G. Handover Delay

We focus on the impact of the handover execution process on the handover latency, thus we set the downlink transmission packet size to 1.7 KB per time slot interval. Figs. 14 and 15 show the average handover delay of aircraft with the different numbers of subchannels and different satellite scales, respectively. It can be seen that the increasing number of subchannels and satellites can effectively reduce the handover delay, and the performance of the PHSU algorithm is optimal. When the number of subchannels continues to increase to 15, the performance obtained by executing algorithms successively shows the limitation of the enhancement, the MD algorithm only considers the link distance index, and does not consider the influence of the subchannel configuration, so the MD algorithm first exhibits the limitation of increasing the number of subchannels to improve the handover delay. The MR algorithm only considers the link rate factor, and the obtained handover performance greatly depends on the channel conditions, so the change in the number of subchannels has the greatest impact on the MR algorithm. With the increase in the subchannel or the expansion of the satellite scale, the PHSU algorithm can decide aircraft to handover to the LEO satellites with better subchannel conditions, thus greatly reducing the transmission delay. The PHSU algorithm considers the effect of co-channel interference so that all aircraft can minimize the effect of interference. Particularly, when the number of satellites is expanded from 4,408 to 11,927, the handover delay obtained by the SD algorithm increases. It is because although new LEO satellites with lower distances are selected, their subchannel conditions are not necessarily improved, which leads to an increase in the handover delay instead. The PHSU algorithm takes into account the various factors affecting the handover delay and has a strong adaptability to the environment, which can be adapted as much as possible to improve the system performance, thus the proposed algorithm demonstrates robustness and adaptability compared to the benchmark algorithms.

VII. Conclusion

In this paper, we have investigated multiple civil aircraft handover issue in UDLSN. First, we have considered different priorities of civil aircraft and have constructed a handover satisfaction function including rate satisfaction, power overhead, and handover overhead as handover criteria. To maximize the handover satisfaction of all aircraft, we have modeled the handover problem as a local cooperative game, in which each aircraft cooperates with other interference aircraft to make the handover decision. We have proved the existence of the NE solution (i.e., local or global optimal solution) for the proposed game and have proposed the PHSU algorithm to find an NE solution. Simulation results have demonstrated that the PHSU algorithm can meet different service levels of aircraft and effectively reduce the handover delay and the handover times, which highlights the superiority of the proposed algorithm in UDLSN. We believe that this study will shed light on the satellite handover for civil aviation and would provide an effective handover algorithm for the application of UDLSN. In the future, we will investigate the LEO satellite handover strategy in the passenger-to-LEO communication scenario by considering the handover failure rate and ping-pong effect.

References

[1] K. Molchanova and M. Semeriahina, *Prospects for the Recovery of the Aviation Industry in Ukraine*. Riga, Latvia: Publishing House Baltija Publishing, 2023.

[2] J. Liu, Y. Shi, Z. M. Fadlullah, and N. Kato, "Space-air-ground integrated network: A survey," *IEEE Commun. Surveys Tut.*, vol. 20, no. 4, pp. 2714–2741, Fourth Quarter 2018.

[3] L. Abouzaid, E. Sabir, H. Elbiaze, A. Errami, and O. Benhmammouch, "The meshing of the sky: Delivering ubiquitous connectivity to ground Internet of Things," *IEEE Internet Things J.*, vol. 8, no. 5, pp. 3743–3757, Mar. 2021.

[4] I. Hatty, "Viability of on-orbit servicing spacecraft to prolong the operational life of satellites," *J. Space Saf. Eng.*, vol. 9, no. 2, pp. 263–268, 2022.

[5] J. C. McDowell, "The low earth orbit satellite population and impacts of the spacex starlink constellation," *Astrophysical J. Lett.*, vol. 892, no. 2, 2020, Art. no. L36.

[6] X. Liu, T. Ma, Z. Tang, X. Qin, H. Zhou, and X. Shen, "UltraStar: A lightweight simulator of ultra-dense LEO satellite constellation networking for 6G," *IEEE/CAA J. Automatica Sinica*, vol. 10, no. 3, pp. 632–645, Mar. 2023.
[7] T. Ma, B. Qian, X. Qin, X. Zhang, N. Cheng, and H. Zhou, "Joint subchannel allocation and beamforming for multicast in ultra-dense LEO backbone network," in *Proc. 2022 IEEE Glob. Commun. Conf.*, 2022, pp. 1625–1630.
[8] H. Zhou, J. Li, K. Yang, H. Zhou, J. An, and Z. Han, "Handover analysis in ultra-dense LEO satellite networks with beamforming methods," *IEEE Trans. Veh. Technol.*, vol. 72, no. 3, pp. 3676–3690, Mar. 2023.
[9] Y. Wang, X. Qin, Z. Tang, T. Ma, X. Zhang, and H. Zhou, "QoS-centric handover for civil aviation aircraft access in ultra-dense LEO satellite networks," in *Proc. 2022 IEEE/CIC Int. Conf. Commun. China*, 2022, pp. 1085–1089.
[10] H. Zhou, H. Zhou, J. Li, K. Yang, J. An, and X. Shen, "Heterogeneous ultra-dense networks with traffic hotspots: A unified handover analysis," *IEEE Internet Things J.*, vol. 10, no. 10, pp. 8825–8838, May 2023.
[11] H. Xu, D. Li, M. Liu, G. Han, W. Huang, and C. Xu, "QoE-driven intelligent handover for user-centric mobile satellite networks," *IEEE Trans. Veh. Technol.*, vol. 69, no. 9, pp. 10127–10139, Sep. 2020.
[12] K. Xue, W. Meng, S. Li, D. S. L. Wei, H. Zhou, and N. Yu, "A secure and efficient access and handover authentication protocol for Internet of Things in space information networks," *IEEE Internet Things J.*, vol. 6, no. 3, pp. 5485–5499, Jun. 2019.
[13] N. M. Kibinda and X. Ge, "User-centric cooperative transmissions-enabled handover for ultra-dense networks," *IEEE Trans. Veh. Technol.*, vol. 71, no. 4, pp. 4184–4197, Apr. 2022.
[14] T. Ma, B. Qian, X. Qin, X. Liu, H. Zhou, and L. Zhao, "Satellite-terrestrial integrated 6 G: An ultra-dense LEO networking management architecture," *IEEE Wireless Commun.*, vol. 31, no. 1, pp. 62–69, Feb. 2024.
[15] P. Du, J. Li, W. Bai, M. Sheng, and D. Zhou, "Dual location area based distributed location management for hybrid LEO/MEO mega satellite networks," *IEEE Trans. Veh. Technol.*, vol. 72, no. 2, pp. 2307–2321, Feb. 2023.
[16] D. Wang, Y. Wang, S. Dong, G. Huang, J. Liu, and W. Gao, "On delay-aware resource control with statistical QoS provisioning by dual connectivity in heterogeneous aeronautical network," *IEEE Trans. Veh. Technol.*, vol. 69, no. 3, pp. 2915–2927, Mar. 2020.
[17] R. Deng, B. Di, H. Zhang, L. Kuang, and L. Song, "Ultra-dense LEO satellite constellations: How many LEO satellites do we need?," *IEEE Trans. Wireless Commun.*, vol. 20, no. 8, pp. 4843–4857, Aug. 2021.
[18] B. Di, H. Zhang, L. Song, Y. Li, and G. Y. Li, "Ultra-dense LEO: Integrating terrestrial-satellite networks into 5G and beyond for data offloading," *IEEE Trans. Wireless Commun.*, vol. 18, no. 1, pp. 47–62, Jan. 2019.
[19] S. Alam, S. Sulistyo, I. W. Mustika, and R. Adrian, "Handover decision for V2V communication in vanet based on moving average slope of RSS," *J. Commun.*, vol. 16, no. 7, pp. 284–293, 2021.
[20] X. Jia, D. Zhou, M. Sheng, Y. Shi, N. Wang, and J. Li, "Reinforcement learning-based handover strategy for space-ground integration network with large-scale constellations," *J. Commun. Inf. Netw.*, vol. 7, no. 4, pp. 421–432, 2022.
[21] W. Qi, Q. Song, S. Wang, Z. Liu, and L. Guo, "Social prediction-based handover in collaborative-edge-computing-enabled vehicular networks," *IEEE Trans. Computat. Social Syst.*, vol. 9, no. 1, pp. 207–217, Feb. 2022.
[22] F. Wang, D. Jiang, Z. Wang, J. Chen, and T. Q. Quek, "Seamless handover in LEO based non-terrestrial networks: Service continuity and optimization," *IEEE Trans. Commun.*, vol. 71, no. 2, pp. 1008–1023, Feb. 2023.
[23] Z. Wu, F. Jin, J. Luo, Y. Fu, J. Shan, and G. Hu, "A graph-based satellite handover framework for LEO satellite communication networks," *IEEE Commun. Lett.*, vol. 20, no. 8, pp. 1547–1550, Aug. 2016.
[24] L. Zhao, C. Wang, K. Zhao, D. Tarchi, S. Wan, and N. Kumar, "INTERLINK: A digital twin-assisted storage strategy for satellite-terrestrial networks," *IEEE Trans. Aerosp. Electron. Syst.*, vol. 58, no. 5, pp. 3746–3759, Oct. 2022.
[25] L. Yiqing, L. Yuqing, G. Xiaoying, W. Jingchao, X. Youyun, and W. Xinbing, "Markov approximation for multilayered selection in satellite network," *J. Commun. Inf. Netw.*, vol. 1, no. 3, pp. 23–31, 2016.
[26] K. Gao, C. Xu, P. Zhang, J. Qin, L. Zhong, and G.-M. Muntean, "GCH-MV: Game-enhanced compensation handover scheme for multipath TCP in 6G software defined vehicular networks," *IEEE Trans. Veh. Technol.*, vol. 69, no. 12, pp. 16142–16154, Dec. 2020.
[27] H. Jiang, H. Wang, Y. Hu, and J. Wu, "Dynamic user association in scalable ultra-dense LEO satellite networks," *IEEE Trans. Veh. Technol.*, vol. 71, no. 8, pp. 8891–8905, Aug. 2022.
[28] Z.-X. Liu, X.-C. Jin, Y.-A. Xie, and Y. Yang, "Joint slot scheduling and power allocation in clustered underwater acoustic sensor networks," *IEEE/CAA J. Automatica Sinica*, vol. 10, no. 6, pp. 1501–1503, 2023.
[29] R. Ruby, S. Zhong, H. Yang, and K. Wu, "Enhanced uplink resource allocation in non-orthogonal multiple access systems," *IEEE Trans. Wireless Commun.*, vol. 17, no. 3, pp. 1432–1444, Mar. 2018.
[30] N. Zhang, S. Zhang, J. Zheng, X. Fang, J. W. Mark, and X. Shen, "QoE driven decentralized spectrum sharing in 5G networks: Potential game approach," *IEEE Trans. Veh. Technol.*, vol. 66, no. 9, pp. 7797–7808, Sep. 2017.
[31] C. Zhang, C. Jiang, J. Jin, S. Wu, L. Kuang, and S. Guo, "Spectrum sensing and recognition in satellite systems," *IEEE Trans. Veh. Technol.*, vol. 68, no. 3, pp. 2502–2516, Mar. 2019.
[32] F. Li, K.-Y. Lam, X. Liu, J. Wang, K. Zhao, and L. Wang, "Joint pricing and power allocation for multibeam satellite systems with dynamic game model," *IEEE Trans. Veh. Technol.*, vol. 67, no. 3, pp. 2398–2408, Mar. 2018.
[33] N.-T. Nguyen and B.-H. Liu, "The mobile sensor deployment problem and the target coverage problem in mobile wireless sensor networks are NP-hard," *IEEE Syst. J.*, vol. 13, no. 2, pp. 1312–1315, Jun. 2019.
[34] D. Monderer and L. S. Shapley, "Potential games," *Games Econ. Behav.*, vol. 14, no. 1, pp. 124–143, 1996.
[35] I. Bistritz and A. Leshem, "Approximate best-response dynamics in random interference games," *IEEE Trans. Autom. Control*, vol. 63, no. 6, pp. 1549–1562, Jun. 2018.
[36] C. Eksin and A. Ribeiro, "Distributed fictitious play for multiagent systems in uncertain environments," *IEEE Trans. Autom. Control*, vol. 63, no. 4, pp. 1177–1184, Apr. 2018.
[37] S. Lhazmir, O. A. Oualhaj, A. Kobbane, and J. Ben-Othman, "Matching game with no-regret learning for IoT energy-efficient associations with UAV," *IEEE Trans. Green Commun. Netw.*, vol. 4, no. 4, pp. 973–981, Dec. 2020.
[38] T. Tatarenko, "Independent log-linear learning in potential games with continuous actions," *IEEE Trans. Control Netw. Syst.*, vol. 5, no. 3, pp. 913–923, Sep. 2018.
[39] Y. Chen, J. Sun, Y. Lin, G. Gui, and H. Sari, "Hybrid N-inception-LSTM-based aircraft coordinate prediction method for secure air traffic," *IEEE Trans. Intell. Transp. Syst.*, vol. 23, no. 3, pp. 2773–2783, Mar. 2022.

Yilei Wang (Graduate Student Member, IEEE) received the B.S. degree in electronic information science and technology from Central South University, Changsha, China, in 2021. She is currently working toward the Ph.D. degree in communications and information system with Nanjing University, Nanjing, China. Her research interests include space-air-ground integrated network, airborne Internet, handover management, and resource allocation.

Ting Ma (Member, IEEE) received the B.S., MS., and Ph.D. degrees in statistics from Sichuan University, Chengdu, China, in 2013, 2016, and 2020, respectively. From 2020 to 2023, she was a Postdoctoral Fellow with the School of Electronic Science and Engineering, Nanjing University, Nanjing, China. She is currently an Associate Professor with the School of Electronic and Optical Engineering, Nanjing University of Science and Technology, Nanjing, China. Her research interests include space-air-ground integrated network, convex optimization theory, robust hypothesis testing, and game theory.

Xiaohan Qin (Student Member, IEEE) received the B.S. degree in communication engineering from Central South University, Changsha, China, in 2020. She is currently working toward the Ph.D. degree in communications and information system with Nanjing University, Nanjing, China. Her research interests include space-air-ground integrated networks, network resource management and game theory.

Xin Zhang (Graduate Student Member, IEEE) received the B.S. degree in mathematics and physics basic science from University of Electronic Science and Technology of China, Chengdu, China, in 2020. She is currently working toward the Ph.D. degree in communications and information system with Nanjing University, Nanjing, China. Her research interests include space-air-ground integrated netowrks, resource allocation, and convex optimization theory.

Zitian Zhang(Member, IEEE) received the B.S. and Ph.D. degrees from Shanghai Jiao Tong University, in 2010 and 2016, respectively. From 2016 to 2017, he was a Research Engineer in China Aeronautical Radio Electronics Research Institute. From 2018 to 2020, he was with East China University of Science and Technology, Shanghai, China. From 2020 to 2022, he was a Mary Curie Research Fellow with the Ranplan Wireless Network Design Ltd. His research interests include deep learning, Big Data analytics, and device-to-device communications.

Haibo Zhou (Senior Member, IEEE) received the Ph.D. degree in information and communication engineering from Shanghai Jiao Tong University, Shanghai, China, in 2014. From 2014 to 2017, he was a Postdoctoral Fellow with the Broadband Communications Research Group, Department of Electrical and Computer Engineering, University of Waterloo, Waterloo, ON, Canada. He is currently a Full Professor with the School of Electronic Science and Engineering, Nanjing University, Nanjing, China. He was the recipient of the 2019 IEEE ComSoc Asia-Pacific Outstanding Young Researcher Award. He was selected as an IEEE ComSoc Distinguished Lecturer for the class from 2023 to 2024. He was a Track/Symposium CoChair for IEEE/CIC ICCC 2019, IEEE VTC-Fall 2020, IEEE VTC-Fall 2021, and IEEE GLOBECOM 2022. He is currently an Associate Editor of the IEEE TRANSACTIONS ON WIRELESS COMMUNICATIONS, IEEE INTERNET OF THINGS JOURNAL, *IEEE Network Magazine*, and IEEE WIRELESS COMMUNICATIONS LETTER. His research interests include resource management and protocol design in B5G/6G networks, vehicular ad hoc networks, and space-air-ground integrated networks.